The Analysis of Heat-Mass Transport and Pressure in Unsaturated Multi-Layered Porous Material under a Combined Infrared and Microwave Energy (Influence of Structures of Multi-Layered)

Sungsoontorn.S[1], Jindarat.W[2] and Rattanadecho.P[2,*]

[1] Department of Mechanical Engineering, Faculty of Engineering,
Rajamangala University of Technology Rattanakosin, 96 Mu 3, Thanon Phutthamonthon Sai 5,
Salaya Phutthamonthon Nakhon Pathom, 73170, Thailand.
[2] Research Center of Microwave Utilization in Engineering (R.C.M.E.)
Department of Mechanical Engineering, Faculty of Engineering,
Thammasat University (Rangsit Campus), Pathumthani 12120, Thailand,
*Corresponding Author: E-mail: ratphadu@engr.tu.ac.th,Tel: 0-2564-3001-9, Fax: 0-2564-3010.

Abstract

In this study, a porous media model was developed to predict heat transfer and moisture transport during a combined infrared and microwave drying of unsaturated multi-layered porous material. A total gas pressure equation was introduced to address internal vapor generation in a combined infrared and microwave drying. The resulting governing equations were numerically solved with the finite volume method. All the physical, thermodynamic, thermal, transport, and dielectric properties used in the multi-layered porous material (composed of glass beads, water and air) either from our measurements or from the literature. From the results showed that the variation of the structures of multi-layered plays an important role on overall drying kinetics. The moisture profile in the unsaturated porous material suggests the importance of capillary flow in combined infrared and microwave drying. The results presented here provide a basis for fundamental understanding of a combined infrared and microwave drying of unsaturated porous materials and can be applied as useful tool for exploring practical problems.

Keywords*:* Unsaturated Porous Material, Particle Size, Combined Infrared and Microwave Energy, Multi-Layered

1. Introduction

The drying process of porous media is a complicated process involving simultaneous, coupled heat and mass transfer phenomena. Modeling simultaneous heat and mass transport in porous media is of growing interest in wide range of new technology. In order to improve process performance and energy utilization for new technologies related to medical application, geothermal analysis, freeze drying processes, forest product, building materials, food stuffs and microwave drying process have been applied. Knowledge of heat and mass transfer that occurs during convective drying of porous materials is crucial to reduce energy cost of drying, equipment and process design, and preserve the quality of

products. The study of heat - mass transfer and gas pressure in the unsaturated porous media is microscopic scale. However, a combined infrared and microwave energy play an important role on overall drying kinetics. Refer to Metaxas and Meredith (1983) and Saltiel and Datta (1997) for an introduction to heat and mass transfers in microwave processing. Other important papers addressing modeling of microwave heating processes include Ayappa et al. (1985), Clemens et al. (1996), Zhao et al. (1998), Basak et al. (2001) and Ratanadecho et al. (2001), Ratanadecho et al. (2002) such as Boukadida et. al., (2002) was study of heated and mass in porous media behaviors is important for temperature, gas pressure and moisture content meanwhile drying processed. Heat and mass transfer in porous materials were carried out empirically but unused microwave. Adonis, (2004) showed numerical modeling of the dynamics of a dryer for food and agricultural products incorporating a combination of convective and infrared radiation. Glouannec, (2002) studied with experimental drying in porous materials by a combination of convection as well as infrared and microwave radiation. Praveen, (2005) studied with the combination of infrared and hot-air drying of onion slices was explored, and the effects of processing conditions such as drying temperature, slice thickness, air temperature and velocity on onion slice characteristics. Salagnac et al. (2004). This study deals with numerical of the hydrothermal behavior of a rectangular-shaped porous material during combined drying. This material is submitted on its upper side both a hot air flow as well as infrared and microwave radiation. Datta and Ni, (2002) studied with temperature and moisture profiles for infrared and hot-air-assisted microwave heating of food were studied using a multiphase porous media transport model for energy and moisture in the food. However, most of previous works deal with the drying of uniform materials. Indeed, little effort has been reported on the study of drying process of non-uniform material i.e., multi-layered material especially a complete comparison between mathematical model and experimental data.

Typical applications of non-uniform material include the tertiary oil recovery process, geothermal analysis, asphaltic concrete pavements process and preservation process of food stuffs. Therefore, knowledge of heat and mass transfer that occurs during a combined infrared and microwave drying of unsaturated multi-layered porous material is necessary to provide a basis for fundamental understanding of a combined infrared and microwave drying of unsaturated multi-layered porous material. This paper contains a useful review, an experimental study of heat and mass transfer in a combined infrared and microwave drying of unsaturated multi-layered porous material, and supporting numerical work. In a recent work, Ratanadecho et al.(2002) carried out the first systematical study on drying process of multi-layered packed bed by a combined infrared and microwave energy, however, no theoretical confirmation is reported. Due to the limited amount of theoretical and experimental work on a combined infrared and microwave drying of unsaturated multi-layered porous material.The effects of particle size and the multi-layered on the overall drying kinetics have not been systematically studied. Although most previous investigations consider single-

layered material, little effort has been reported on a combined infrared and microwave energy of multi-layered material (non-uniform structure) at a fundamental level, especially, full comparison between mathematical simulation results and experimental drying data.

2. Mathematical formulation

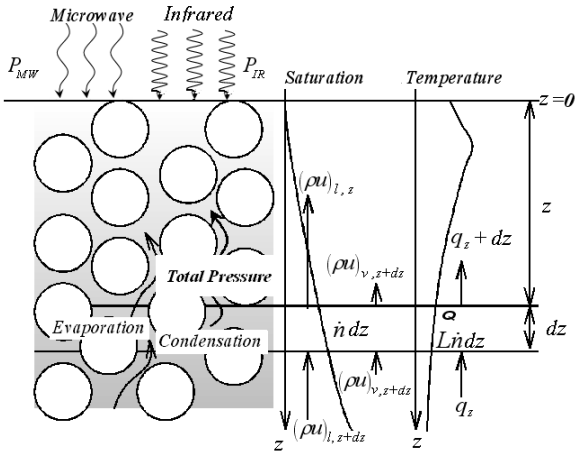

Figure 1. Analytical model.

Figure 1 shows the analytical model for combined infrared and microwave drying of the sample. As shown in figure 2, the samples are unsaturated packed beds composed of glass beads, water and air. The samples are prepared in the configurations in the multi-layered porous media. The multi-layered porous media are arranged in different configurations in the fine–coarse bed ,F-C bed (fine particles (an average diameter of 0.15 mm, δ =10 mm) is over the coarse particles (an average diameter of 0.4 mm, δ =10 mm)) (Figure 2(a)) and the coarse-fine bed ,C-F bed (coarse particles (an average diameter of 0.4 mm, δ =10 mm)) is over the fine particles (an average diameter of 0.15 mm, δ =10 mm)) (Figure 2(b)), respectively.

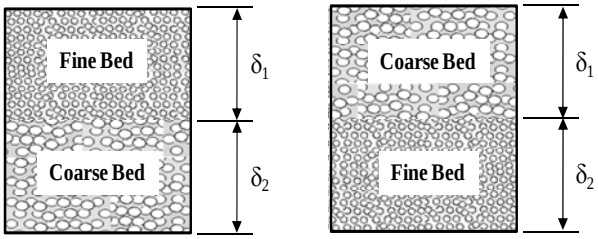

(a) (b)

Figure 2 Multi-layered porous media (Sample):
(a) Multi-layered porous media: Fine-Coarse Bed.(F-C bed)
(b) Multi-layered porous media: Coarse-Fine Bed (C-F bed).

The rate of volumetric energy absorbed corresponding to the microwave absorbed energy was assumed to decay exponentially into the sample, according to Lambert's law. The basic equation to calculate the density of microwave power absorbed by dielectric material can be written in the final form as: (Ratanadecho et al.(2001))

$$Q_j = -\frac{\partial P}{\partial z}dz = 2\alpha P dz = 2\alpha dz.2\pi f\varepsilon_j(\tan\delta)_j E^2 e^{-2\alpha z} \quad (1)$$

where E is the electromagnetic field intensity; f is the frequency of the microwave; ω is the angular velocity of the microwave; $tan\delta$ is the dielectric loss tangent coefficient; α is the attenuation constant, which can be calculated from: (Ratanadecho et al.(2001)) The attenuation parameter (α) controls the rate at which the incident field decays, and is inversely proportional to the skin depth, i.e., $\alpha = 1/\delta_s$. In this work, the effects of the overall drying kinetics are examined by selecting the dielectric properties as a function of water saturation (moisture content) and temperature, the theory mixing the formulas by Wang and Schmugge (1980) is used.The loss tangent coefficient can be expressed as follows:

$$\tan \delta_j = \frac{\varepsilon_r''}{\varepsilon_r'} \quad (3)$$

where ε_r'' is a relative dielectric loss factor and ε_r' is a relative dielectric constant.

The main transport mechanisms that enable moisture movement during the combined infrared and microwave drying of the sample are liquid flows driven by capillary pressure gradient and gravity. However, the vapor is driven by the gradient of the partial pressure of the evaporating species. The main assumptions involved in the formulation of the transport model are:

1. The capillary porous material is rigid. No chemical reactions occur in the sample.
2. The local thermodynamics equilibrium among each phase is assumed.
3. The gas phase is ideal in the thermodynamic sense.
4. The contribution of convection to energy transport is included.
5. Darcy's law holds valid for the liquid and gas phases.
6. Gravity is included particularly in the liquid and gas phases.
7. The permeability of liquid and gas can be expressed in terms of relative permeability.
8. In a macroscopic sense, the packed bed is assumed to be homogeneous and isotropic, and liquid water is not bound to the solid matrix. Therefore, the volume average model for a homogeneous and isotropic material can be used in the theoretical model and analysis.
9. Corresponding to the electric field, the temperature and moisture profiles are assumed to have a one-dimensional form.
10. The microwave absorbed energy is assumed to decay exponentially into the sample, according to Lambert's law.
11. The non-thermal effect of microwave irradiation is neglected.

2.1 Heat Transport Equation

The kinetic energy and pressure terms, which are usually unimportant are ignored. Local thermodynamics equilibrium among all phases is assumed. The temperature of unsaturated porous media is obtained by solving the conventional heat transport equation. Considering the enthalpy transport based on the water and gas flows, the conduction heat and latent heat transfer are due to evaporation. The energy conservation equation is represented by:

$$\frac{\partial}{\partial t}\left(\left(\rho C_p\right)_{T,j} T\right)+\frac{\partial}{\partial z}\left(\left(\rho_l C_{pl} w_{l,j}+\left(\rho_a C_{pa}+\rho_v C_{pv}\right)w_{g,j}\right)T\right)=\frac{\partial}{\partial z}\left(\lambda_{eff\ j}\frac{\partial T}{\partial z}\right)$$
$$-H_v\left(\frac{\partial}{\partial t}\left(\rho_v \phi_j\left(1-s_j\right)\right)+\frac{\partial}{\partial z}\left(\rho_v \frac{K_j K_{rg}}{\mu_g}\left(-\frac{\partial P_g}{\partial z}+\rho_g g_z\right)-\rho_g D_{mj}\frac{\partial}{\partial z}\left(\frac{\rho_v}{\rho_g}\right)\right)\right)$$
$$+Q_{MWj}+Q_{IRi} \quad (4)$$

2.2 Mass Transport Equation

The phenomenon of moisture transport is described by the mass conservation equations for the liquid phase and for the water vapor in the gas phase since the total water content is of interest. The addition of those one dimensional equations and yields total moisture content as follows:

$$\phi_j \frac{\partial}{\partial t}\left\{Y_v\left(1-s_j\right)\right\}+\frac{\partial}{\partial z}\left[\frac{K_j K_{rlj}}{\mu_l}\left(\frac{\partial P_c}{\partial z}-\frac{\partial P_g}{\partial z}+g_z\right)+Y_v\frac{K_j K_{rgj}}{\mu_g}\left(-\frac{\partial P_g}{\partial z}+\rho_g g_z\right)-Y_g D_{mj}\frac{\partial}{\partial z}\left(W_v\right)\right]=0 \quad (5)$$

where $\frac{\rho_v}{\rho_l}=Y_v$, $\frac{\rho_g}{\rho_l}=Y_g$, $\frac{\rho_a}{\rho_l}=Y_a$, $\frac{Y_v}{Y_g}=W_v$

2.3 The Pressure Buildup in Porous Media Equation

The pressure buildup in the porous media is obtained from air-balance equation as follows:

$$\phi_j \frac{\partial}{\partial t}\left\{Y_a\left(1-s_j\right)\right\}+\frac{\partial}{\partial z}\left[Y_a \frac{K_j K_{rgj}}{\mu_g}\left(-\frac{\partial P_g}{\partial z}+\rho_g g_z\right)-Y_g D_m \frac{\partial}{\partial z}\left(\frac{\rho_a}{\rho_g}\right)\right]=0 \quad (6)$$

2.4 Boundary and Initial Conditions

The boundary conditions proposed for the open boundary of the sample define the exchange of energy at the open boundary which can be described in the following form:

$$-\lambda_{eff\ j}\frac{\partial T}{\partial z}=h_c\left(T-T_a\right)+\dot{n}H_v$$

$$\rho_l w_{l,j}+\rho_v w_{v,j}=h_m\left(\rho_v-\rho_{va}\right) \quad (7)$$

where h_c is the heat transfer coefficient , h_m is the mass transfer coefficient, ρ_v is the density of water vapor at the open boundary and ρ_{va} is reference vapor density in the gas phase surrounding the open boundary. The boundary conditions at the symmetrical impermeable surface are given by:

$$\frac{\partial T}{\partial z}=0,\quad \frac{\partial w_l}{\partial z}=\frac{\partial w_a}{\partial z}=\frac{\partial w_v}{\partial z}=0 \quad (8)$$

From a macroscopic point of view, we will consider liquid water transport at the interface between two beds where the difference in particle size is considered. The capillary pressure, mass transfer and temperature are assumed to be continuous at the interface of layered packed bed:

$$P_{c,F}=P_{c,C}\,,\ \rho_l w_{l,F}=\rho_l w_{l,C}\,,$$

$$\rho_g w_{g,F}=\rho_g w_{g,C}\,,\ T_F=T_C \quad (9)$$

3.Numerical technique

The heat, mass transfer and total pressure equations were coupled to the Lambert's law for find all phenomena within the sample. In order to predict heat, mass transfer and total pressure equations, a finite difference based on control volumes as describe by Patankar.,1980, was applied. The details of the computational schemes and strategy are illustrated in figure 3. The electromagnetic and thermo-physical properties for multi-layered porous (F-C bed and C-F bed) used in the computation are given in table 1.

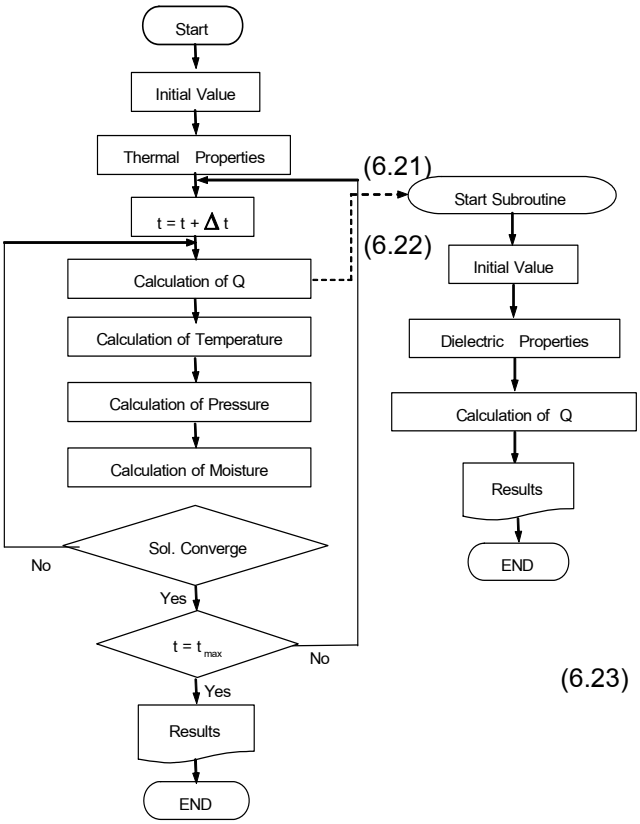

Figure 3. Computational scheme.

Table 1. The electromagnetic and thermo-physical properties used in the computations.

$\varepsilon_0 = 8.85419 \times 10^{-12}$ [F/m]	$\varepsilon_{ra} = 1.0$	$\varepsilon_{rp} = 5.1$
$\mu_0 = 4.0\pi \times 10^{-7}$ [H/m]	$\mu_{ra} = 1.0$	$\mu_{rp} = 1.0$
$\mu_{rl} = 1.0$	$\tan\delta_a = 0.0$	$\tan\delta_p = 0.01$
$\rho_a = 1.205$[kg/m^3]	$\rho_p = 2,500$ [kg/m^3]	$\rho_l = 1,000$ [kg/m^3]
$C_{pa} = 1.007$[kJ/(kg·K)]	$C_{pp} = 0.80$[kJ/(kg·K)]	$C_{pa} = 4.186$[kJ/(kg·K)]
λ_a[W/(m·K)]	$\lambda_p = 1.0$[W/(m·K)]	$\lambda_l = 0.610$[W/(m·K)]
Initial saturation (s) = 0.7	$T_{air} = 30^0$C	
htc = 15[W/(m^2·K)]	hr = 0.58[m/s)]	

4. Results and discussion

The porous material is directly related to the water saturations in the packed bed. The Water saturation is defined as the fraction of the ratio of water volume to pore volume that means the large particle size (C bed) have low water saturation. This is the space among the large particles is smaller than the small particle (F bed). Then the water content, inside the packed bed that contains large particles, is lower than the packed bed that contains small particles. The a combined infrared and microwave energy absorbed, the temperature profiles, the moisture profiles and pressure distribution are shown in figures 4, 5, 6 and 7, respectively. Figure 6 shows the moisture profiles for multi-layered porous media (Fine-Coarse Bed; F-C bed and Coarse-Fine Bed; C-F bed), based on the frequency 2.45 GHz, electric field intensity 4,200 V/m and initial moisture content 0.5. The observed moisture profiles near the heated edge of the sample in the case of small particle size are higher than the others since a higher capillary force causes moisture to reach the surface at a higher rate than the case of large particle size (C bed) due to the a combined infrared and microwave energy absorbed (figure 6.4). The following discussion refers to the effect of glass bead size under the same conditions. In more detail, the liquid water is migrated from the C bed to F-bed via the interface has the same capillary pressure at the interface. Therefore, F-bed has higher dielectric properties than C-bed. Form this point, the a combined infrared and microwave energy absorbed with higher energy absorbed is formed at C-bed, which has lower dielectric properties, while the energy absorbed with smaller energy absorbed is formed at F-bed, which has higher dielectric properties. The multi-layered porous media: Fine-Coarse Bed (F-C bed) has high power absorbed inside top layer (F bed) and multi-layered porous media: Coarse-Fine Bed (C-F bed) has high power absorbed inside bottom layer (F bed).This phenomenon directly affects on heat and mass and pressure buildup in patterns inside both of the layers. Figure 5 shows the temperature profiles at various particle sizes. It is found that the temperature of the small particle (F bed) is higher than the large particle (C bed) in every case of drying time, because the higher moisture content for the small particle (F bed) case and hence larger a combined infrared and microwave energy is absorbed. The both F-C bed and C-F bed results show that a combined infrared and microwave energy induces the higher temperature inside the sample than the surface. That is because a combined infrared and microwave energy can transmitted directly into the sample and transformed to thermal energy inside the sample by itself. However, temperature profile between F-C bed and C-F bed are different. This affect leads C-F bed case to higher temperature than F-C bed case. Figure 6.7 shows that total pressure is much higher, when a long drying time is reached. Figures 8 and 9 depict the fluid movement patterns within the sample, as a function of depth at the forth and tenth hours respectively. The vector profile presented has an advantage of better clarification over the directions and magnitudes. In the figures 8a) and 8b), at the forth hour, the vapor and liquid flow in both directions with the different orders of magnitude, since liquid vaporizes while vapor condenses along its path. In addition, the result of the small particle size (F bed) has a larger flux

than the larger particle size (C bed) does. (The ratios of grid units to magnitude in the case of small particle size (F bed) and in the case of larger particle size (C bed) are 30 and 65 respectively.) However, the air flux of Fine-Coarse Bed (F-C bed) moves towards the surface but in the case of Coarse-Fine Bed (C-F bed) the air flows in the opposite direction because of the effect of capillary pressure. Figure 9a) describes the flux profile of Fine-Coarse Bed (F-C bed) size at the tenth hour. It was found that the vapor flows throughout, and has a higher rate near the central region into which it migrates, in the direction of decreasing saturation. In the case of Coarse-Fine Bed (C-F bed) (figure 9b)) the vapor and liquid flow in the opposite directions, as observed previously. The larger the particle size (C bed) (which corresponds to a higher moisture profile, as referred to figure 6) causes moisture transport to upward at a lower rate than that in the case of small particle size (F bed).

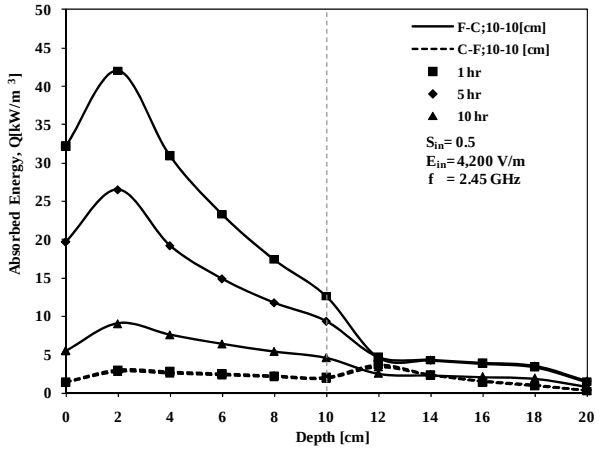

Figure 4 Energy absorbed profiles at various particle size.

(f = 2.45 GHz, E_{in} = 4,200 V/m, Sin = 0.5)

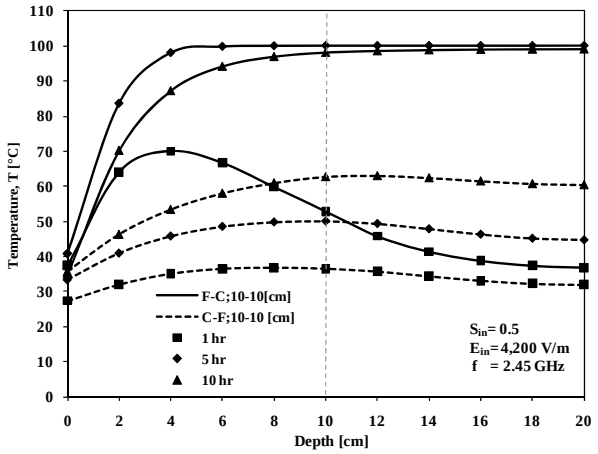

Figure 5 Temperature profiles at various particle size.

(f = 2.45 GHz, E_{in} = 4,200 V/m, Sin = 0.5)

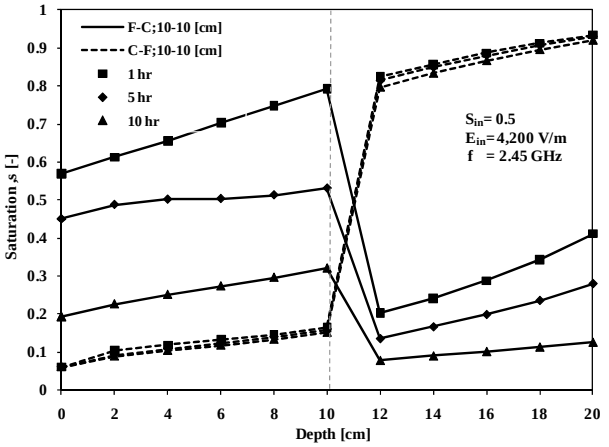

Figure 6 Moisture profiles at various particle size.

(f = 2.45 GHz, E_{in} = 4,200 V/m, Sin = 0.5)

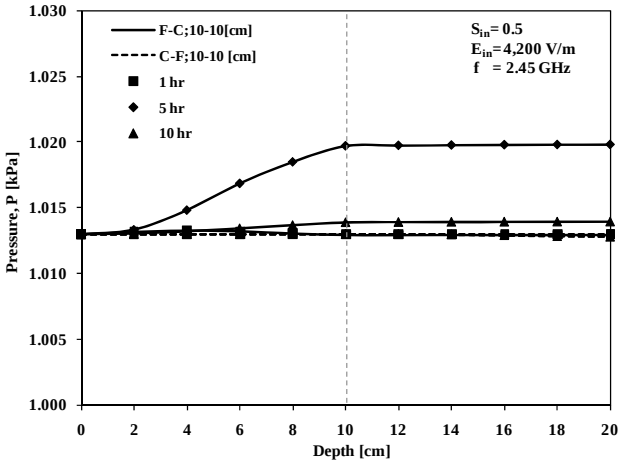

Figure 7 Pressure distribution at various particle size.

(f = 2.45 GHz, E_{in} = 4,200 V/m, Sin = 0.5)

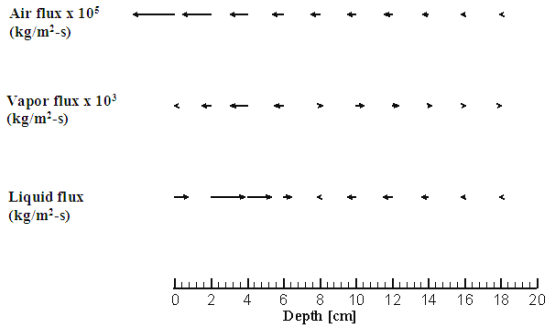

(a)

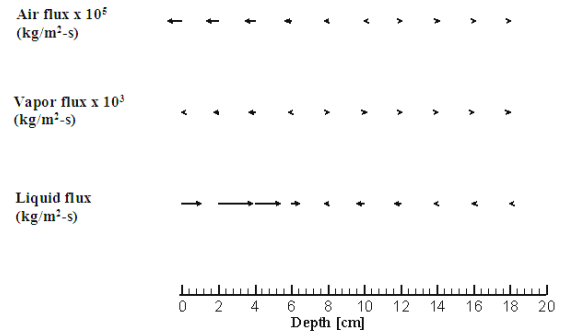

(b)

Figure 8 Fluid movement pattern at 4 hour in case with particle size.

(a) F-C;10-10 cm

(b) C-F;10-10 cm

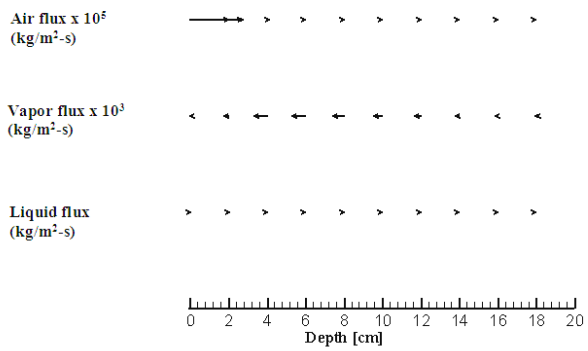

(a)

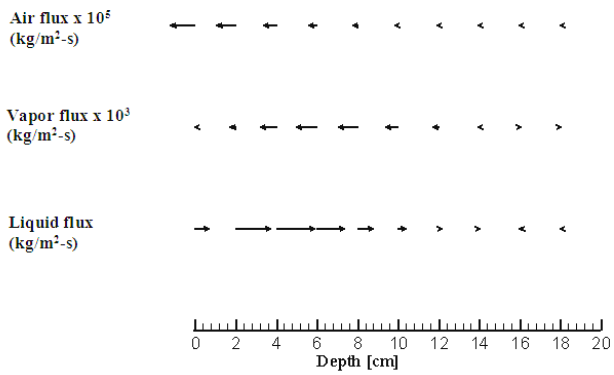

(b)

Figure 9 Fluid movement pattern at 10 hour in case with particle size.

(a) F-C;10-10 cm

(b) C-F;10-10 cm

5. Conclusions

The result presented here provides a basis for fundamental understanding of the combined infrared and microwave drying in porous media. The experiments and theoretically analysis presented in this work describe many of the important interactions within a capillary porous material during the combined infrared and microwave drying. The following summarizes the conclusions of this work:

(1) A generalized mathematical model of drying by microwave oven is proposed. It is used successfully to describe the drying phenomena under various conditions.

(2) The effects of the irradiation time, particle sizes on the combined infrared and microwave drying kinetics is clarified in detail, considering the influence the vapor diffusion and capillary flow.

(3) The small bead size leads to much higher capillary forces resulting in a faster drying time.

6. Acknowledgement

The authors would like to thank the Office of the Higher Education Commission, Thailand, for supporting by grant fund under the program Strategic Scholarships for Frontier Research Network for the Joint Ph.D. Program Thai Doctoral degree and Rajamangala University of Technology Rattanakosin for this research.

7. References

[1] A.C. Metaxas and R.J. Meridith, Industrial Microwave Heating, Peter Peregrinus, Ltd., London, (1983).

[2] C. Saltiel and A.K. Datta, Heat and Mass Transfer in Microwave Processing, Adv. Heat Transfer, 30,1-94, (1997).

[3] K.G. Ayappa, S. Brandon, J.J. Derby, H.T. Davis and E.A. Davis, Microwave Driven Convection in a Square Cavity, AIChE J., 31(5), 842-848, (1985).

[4] J. Clemens and C. Saltiel, Numerical Modeling of Materials Processing in Microwave Furnaces, Int. J. Heat and Mass Transfer, 39(8), 1665-1675, (1996).

[5] H. Zhao, I.W. Turner and G. Torgovnikov, An Experimental and Numerical Investigation of the Microwave Heating of Wood, J. Microwave Power and Electromagnetic Energy, 33, 121-133, (1998).

[6] T. Basak and K.G. Ayappa, Influence of Internal Convection During Microwave Thawing of Cylinders, AICHE Journal, 47, 835-850, (2001).

[7] P. Ratanadecho, K. Aoki and M. Akahori, Influence of Irradiation Time, Particle Sizes and Initial Moisture Content During Microwave Drying of Multi-Layered Capillary Porous Materials, ASME J. Heat Transfer, Vol. 124 (1), 151-161, (2002).

[8] P. Ratanadecho, K. Aoki and M. Akahori, Experimental and Numerical Study of Microwave Drying in Unsaturated Porous Material, Int. Commune, Heat Mass Transfer, 28, 605-616 (2001).

[9] N. Boukadida, S. Ben Nasrallah and P. Perre., Mechanism of Heat and Mass Transfer during Convective Drying of Porous Media under Different Drying Conditions, Drying Technology. 18, 1367-1388, (2000).

[10] M. Adonis, Khan, MTE, Combined Convective and Infrared Drying Model for Food Applications, IEEE AFRICON, 1049-1052 (2004).

[11] P. Glouannec, et al., Experimental Survey on The Combination of Radiating Infrared and Microwave Sources for the Drying of Porous Material, Applied Thermal Engineering, 22, 1689 - 1703 (2002).

[12] D.G. Praveen, et al., Infrared and Hot-Air Drying of Onions, Journal of Food Processing and Preservation, 29, 132-150 (2005).

[13] P. Salagnac, et al., Numerical Modeling of Heat and Mass Transfer in Porous Medium During Combined Hot Air, Infrared and Microwaves Drying, International Journal of Heat and Mass Transfer, 47, 4479–4489 (2004).

[14] A.K.Datta, H. Ni, Infrared and hot-air-assisted microwave heating of food for control of surface moisture, Journal of Food Engineering, 51, 355-364 (2002).

Nomenclature

D_m = effective molecular mass diffusion (m^2/s)

H_v = specific heat of vaporization (J/kg)

E = electric field intensity (V/cm)

Q_{MW} = microwave power absorbed term (W/m^3)
Q_{IR} = Infrared power absorbed term (W/m^3)
ε' = permittivity or dielectric constant
μ_l = dynamic viscosity of liquid (Pa s)
ε'' = dielectric loss factor
μ_g = dynamic viscosity of gas (Pa s)
h_c = heat transfer constant (W/ m^{2}K)
h_m = mass transfer constant (W/ m^{2}K)
λ =effective thermal conductivity (W/mK)
$\dot{n}$ = phase change term (kg/m3s)
w = velocity (m/s)
f = frequency (GHz)
P = microwave power (W)
p = pressure (Pa)
K = permeability (m^2)
$tan\delta$ = loss tangent coefficient
ϕ = Porosity
g = gravitational constant (m/s^2)
ρ = density (kg/m^3)
ε = complex permittivity (F/m)
μ = magnetic permeability (H/m)
t = time (s)
S = water saturation
T = temperature ($^\circ$C)
ε = complex permittivity (F/m)
ε'' = dielectric loss factor
μ_g = dynamic viscosity of gas (Pa s)

g = gas
l = liquid water
x = coordinate axis[m]

Subscripts

0 = free space
p = particle
a = air
r = relative
c = capillary
v = water vapor